Bisphosphonate-adsorbed ceramic nanoparticles increase bone formation in an injectable carrier for bone tissue engineering

Tegan L Cheng[1,2], Ciara M Murphy[1,2], Roya Ravarian[3], Fariba Dehghani[3], David G Little[1,2] and Aaron Schindeler[1,2]

Abstract

Sucrose acetate isobutyrate (SAIB) is a sugar-based carrier. We have previously applied SAIB as a minimally invasive system for the co-delivery of recombinant human bone morphogenetic protein-2 (rhBMP-2) and found synergy when co-delivering zoledronic acid (ZA) and hydroxyapatite (HA) nanoparticles. Alternative bioceramics were investigated in a murine SAIB/rhBMP-2 injection model. Neither beta-tricalcium phosphate (TCP) nor Bioglass (BG) 45S5 had a significant effect on bone volume (BV) alone or in combination with the ZA. ^{14}C-labelled ZA binding assays showed particle size and ceramic composition affected binding with nano-HA > micro-HA > TCP > BG. Micro-HA and nano-HA increased BV in a rat model of rhBMP-2/SAIB injection (+278% and +337%), and BV was further increased with ZA–adsorbed micro-HA and nano-HA (+530% and +889%). These data support the use of ZA–adsorbed nanoparticle-sized HA as an optimal additive for the SAIB/rhBMP-2 injectable system for bone tissue engineering.

Introduction

A key aim of bone tissue engineering research is to develop bone graft substitutes that can repair bone defects without the need for allografts or autografts. There are several approaches to creating effective graft substitutes, which include the delivery of growth factors and/or cells.[1] In terms of biological growth factors, recombinant human bone morphogenetic protein-2 (rhBMP-2) has been a major component of many modern bone tissue engineering solutions and is currently in clinical use. The Food and Drug Administration (FDA) have approved rhBMP-2 for the treatment of lumbar spinal fusion, open fractures of the tibia and sinus augmentation.[2] Clinical delivery of rhBMP-2 is via an absorbable collagen sponge, which leads to difficulties in achieving an optimal release profile.[3] Poor

control over spatiotemporal release of rhBMP-2 can result in unwanted ectopic bone formation or premature local

[1]Orthopaedic Research and Biotechnology Unit, The Children's Hospital at Westmead, Westmead, NSW, Australia
[2]Discipline of Paediatrics and Child Health, Sydney Medical School, University of Sydney, Sydney, NSW, Australia
[3]School of Chemical and Biomolecular Engineering, University of Sydney, Sydney, NSW, Australia

Corresponding author:
Tegan L Cheng, Orthopaedic Research and Biotechnology Unit, The Children's Hospital at Westmead, Research Building, Locked Bag 4001, Westmead, NSW 2145, Australia.
Email: tegan.cheng@sydney.edu.au

bone resorption.[4–6] Consequently, economic and efficacy benefits may result from research into delivery systems that can better restrict rhBMP-2 release and/or reduce the amount of recombinant protein required.[7,8]

We have validated sucrose acetate isobutyrate (SAIB) as an effective system for the minimally invasive delivery of rhBMP-2 and other additives.[9] SAIB is a highly viscous-mixed sucrose ester and demonstrates properties of a semisolid material.[10] The addition of 10%–20% ethanol or other solvents significantly lowers the viscosity, allowing for injection, and the rapid dispersal of solvent after injection causes SAIB to phase transition back to a semisolid state. SAIB is highly biocompatible, having been used as a food additive for over 50 years[11] and more recently as a drug delivery system.[10,12,13]

The use of anti-resorptive agents such as bisphosphonates to increase the retention of new bone is well established, and synergy has been shown with rhBMP-2.[14–17] In a SAIB-rhBMP-2 intramuscular injection model, the addition of the bisphosphonate zoledronic acid (ZA) led to significant increases in bone volume (BV).[9] Further increases in BV were seen with the incorporation of hydroxyapatite nanoparticle (nano-HA) as a colloid suspension within the SAIB carrier.[9] HA is a primary crystalline mineral found in bone and can lead to enhancement of bone matrix mineralisation.[15,18] When delivered with SAIB-rhBMP-2 and ZA, inclusion of HA bound and attenuated the burst release of the ZA.[9,16]

HA was a natural choice for initial studies with SAIB-rhBMP-2 as it is commonly used in orthopaedics as a bone void filler and implant coating.[19–22] However, other bioceramics were speculated to have potential as additive agents. Tricalcium phosphate (TCP) is also available commercially as a bone graft agent and bone substitute.[23–25] Bioglass (BG) is a silicate-based material also used as a bone graft substitute, particularly in the dental field.[26,27] The first aim of this study was to explore the application of TCP and BG in the SAIB-rhBMP system, both in the presence and absence of ZA.

In addition to considering the bioceramic type, the particle size is also a factor that will influence drug binding and bioresorption. In bone tissue engineering context, smaller bioceramic particle sizes have also been associated with increased resorption and osteoclast activity.[28] However, decreasing particle size is associated with an increased surface area-to-volume ratio, which influences the extent for bisphosphonate binding. Thus, a second aim was to investigate the impact of the particle size of a bioceramic on bisphosphonate binding and in functional in vitro and in vivo models.

Methods and materials

Chemicals and pharmaceuticals

The INFUSE® bone graft kit (clinical-grade rhBMP-2) was purchased from Medtronic Australasia for research purposes (North Ryde, NSW, Australia). Carrier-free ZA

Table 1. List of bioceramic particles.

Bioceramic type	Referred to in text as	Particle size
β-Tricalcium phosphate	TCP	5–10 μm
Bioglass 45S5	BG	5–10 μm
Nanoparticle-sized hydroxyapatite	Nano-HA	100 nm
Microparticle-sized hydroxyapatite	Micro-HA	50–150 μm

was purchased from Axxora, LLX (San Diego, CA, USA). Radiolabelled ZA (^{14}C-ZA, specific activity 6.573 MBq/mg) was a gift from Dr J Green (Novartis Pharma AG, Basel, Switzerland). β-TCP particles (average particle size: 5–10 μm) were ground from stock supplies purchased from Sigma–Aldrich (Castle Hill, NSW, Australia; Table 1). BG 45S5 particles were ground from stock (average particle size: 5–10 μm) purchased from Biometic (Sydney, NSW, Australia). Nano-HA (average particle size: 100 nm) and micro-HA (particle size range: 50–150 μm) were purchased from Berkeley Advanced Biomaterials (Berkeley, CA, USA).

SAIB was purchased from Sigma–Aldrich. A stock solution of SAIB was prepared at a dilution of 80:20 SAIB:ethanol and allowed to fully mix overnight on the day prior to surgery. Agents including rhBMP-2, bioceramic particles and ZA (pre-adsorbed to bioceramic particles and air-dried) were added immediately prior to injection.

Animal purchase, housing and ethics

Eight-week-old female C57BL6 mice and 9-week-old male Wistar rats were purchased from the Animal Resources Centre (Perth, WA, Australia) and were kept onsite at the specific pathogen-free (SPF) animal facility. Animals had unrestricted access to chow and water. Prior to surgery, animals were allowed to acclimatise to the facility for a week. Ethics for the experiment was approved by the Children's Hospital at Westmead (CHW)–Children's Medical Research Institute (CMRI) Animal Ethics Committee (Protocol number K294).

Intramuscular injection of SAIB

Ectopic bone was generated in the hind limb of mice using previously published methods.[9] A SAIB-rhBMP-2 solution (20 μL/leg) was injected into the quadriceps muscle of anesthetised mice using a 27G needle. Each mouse received 5 μg rhBMP-2 ± 1 μg ZA ± 2% (w/v) bioceramic. The values for rhBMP-2, ZA and HA were based on the previous studies.[9,29] This model was upscaled to a rat, with 200 μL/rat being injected using a 25G needle, with drug doses being 5 μg rhBMP-2 ± 2 μg ZA ± 2% (w/v) HA. In the rat studies, values for rhBMP-2, ZA and HA were based on the previous work.[30]

In both studies, rodents received post-operative monitoring and were euthanised using a CO_2 gas chamber at 3 weeks (mice) or 4 weeks (rats) after surgery. Muscle tissue containing ectopic bone was dissected and fixed with 4% paraformaldehyde for 4 h at room temperature and then overnight at 4°C and stored in 70% ethanol.

Radiographic analysis

Bone nodule formation was monitored using digital X-ray (Faxitron X-ray Corp, Lincolnshire, IL, USA), including an end-point X-ray at harvest (25 kV, 2× magnification). Samples in the mouse study were next scanned via micro-computed tomography (μ-CT) using a SkyScan 1174 compact μ-CT scanner (Skyscan, Kontich, Belgium). Samples were scanned in 70% ethanol, using a 0.5-mm aluminium filter, 50 kV X-ray tube voltage and 800 μA tube electric current. Bone pellets were scanned at a pixel resolution of 14.8 μm. Rat samples were scanned on a Quantum FX μ-CT scanner (PerkinElmer, Waltham, MA, USA). Samples were scanned using 90-kV X-ray and 80 μA current, at a field of view of 20 mm, resulting in an image pixel size of 40 μm. The scanned images were reconstructed using NRecon (SkyScan) and analysed with the accompanying software package CTAnalyser (version 1.13.5.0; SkyScan).

In vitro binding assay

To determine the affinities of the bisphosphonate ZA for bioceramics, a 50 μM dose of ^{14}C-ZA was added to 2% w/v ceramic particles (HA, TCP and 45S5) in saline and agitated. After 2 h, samples were spun down in a centrifuge and the supernatant carefully extracted and added to scintillation fluid. Radio counts were read in duplicate using a 1900CA Tri-carb liquid scintillation analyser (Packard BioScience, Meriden, CT, USA). Scintillation fluid alone was used as blank control, and a 50 μM dose of ^{14}C-ZA was added directly to scintillation fluid as a positive control. The values measured in the supernatant values were subtracted from positive controls to generate the amount of ^{14}C-ZA that was left bound to the ceramics.

In vitro cell culture assay

The ability for the bioceramics to bind ZA and protect cells from ZA-mediated cytotoxicity was evaluated in the pre-osteoblastic cell line, MC3T3-E1, as previously described.[9] Cells were cultured in α-minimum essential medium (MEM) supplemented with 10% foetal bovine serum, 1% L-glutamine, and 2% penicillin or streptomycin. Cell media was changed every 4 days, and cells were passaged using trypsin-ethylenediaminetetraacetic acid (EDTA). Cells were treated with a cytotoxic dose of 50 μM.[9,31] Transwell inserts (Merck-Millipore, Hesse, Germany; pore size: ~1 μm) were used to allow the ZA-containing media to interact with the ceramic particles without coming into direct contact with the pre-osteoblasts. It was noted that the nano-HA did not pass through the membranes, and this was likely due to the formation of aggregate particles. The inserts were introduced into the well containing cells and media and contained the following treatments: media alone, 2% ceramics, 50 μM ZA or a combination of the ceramic and ZA treatment. For the TCP and BG experiments, n = 1 was performed due to low intra-well variability seen in previous studies;[9] however, n = 3 was used for HA studies.

Cell viability was measured at 7 days post seeding using the Muse cell count and viability assay (Merck-Millipore) as per the manufacturer's instructions. Briefly, cells were trypsinised and re-suspended in media and then added to the assay media. Samples were then vortexed immediately prior to reading by the muse cell analyser.

Fluorescent tartrate-resistant acidic phosphatase staining

Non-decalcified samples were bisected, with one half embedded face down using Tissue Tek OCT Compound (Sakura, Japan) in preparation for cyrosection. Sections of 5 μm thick were cut using cryofilm (Type 2C; Section-Lab, Hiroshima, Japan). Slides were stained for fluorescent tartrate-resistant acidic phosphatase (TRAP) and counterstained using 4′,6-diamidino-2-phenylindole (DAPI). Fluorescence was visualised using Leica SP5 Confocal microscope (Leica Microsystems, Wetzlar, Germany), with emission wavelengths of 460 nm (DAPI) and 555 nm (TRAP). Image capture settings were retained for all samples.

The other half of the bone nodule was decalcified using 0.34 M EDTA and processed for paraffin histology. Samples were cut to 5-μm sections on a Leica RM 2155 microtome (Leica Microsystems) and stained with standard haematoxylin and eosin.

Statistical analysis

Statistical analyses on cell culture results were carried out using the Student's t-test or analysis of variance (ANOVA). In vivo bone formation assays have been previously seen to not follow a normal distribution; thus non-parametric Kruskal–Wallis and post hoc Mann–Whitney U tests were employed. All tests were performed on GraphPad Prism (Version 5.00 for Windows; GraphPad Software, San Diego, CA) with statistical significance set at α < 0.05.

Results

rhBMP-2-SAIB-induced bone is not enhanced by TCP or BG

The capacity of alternative bioceramics β-TCP and BG 45S5 to enhance rhBMP-2-SAIB-induced bone formation
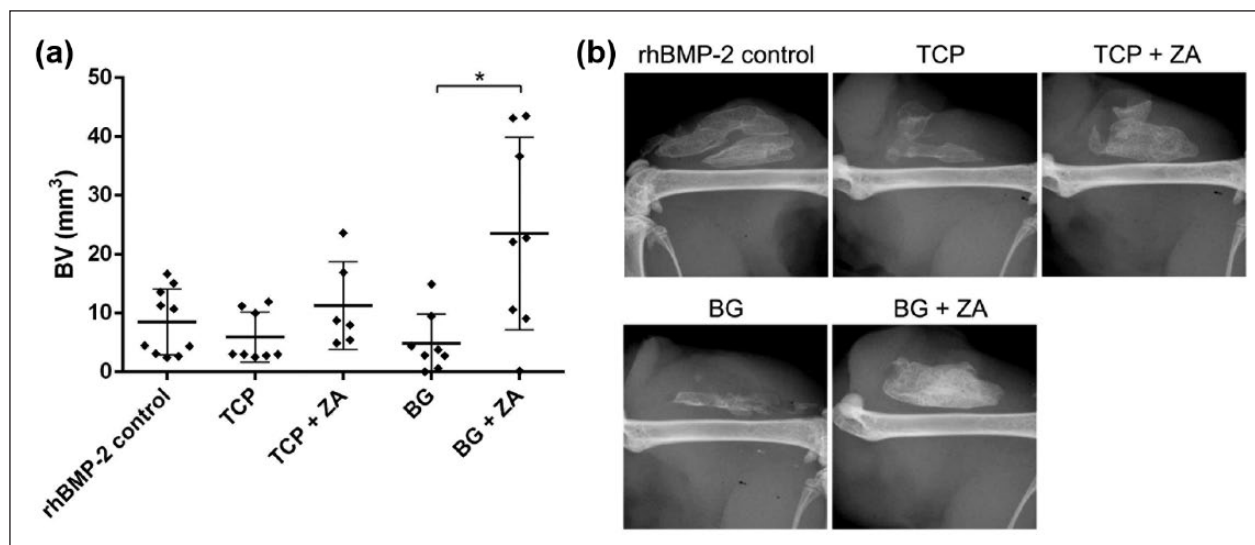
Figure 1. Bone volume (BV) formed in the ectopic mouse muscle pouch model in response to the addition of 5 μg rhBMP-2 is not significantly increased by the addition of either 2% w/v TCP or BG particles, even with the addition of 1 μg ZA: (a) BV of the ectopic nodules quantified by μ-CT and (b) representative X-rays from each group.
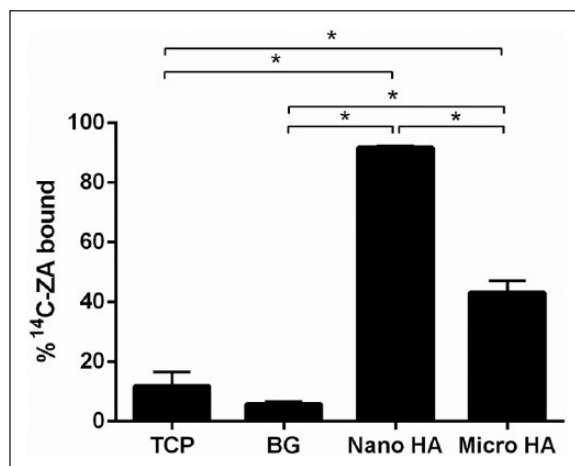$*p < 0.05$.

was measured in an established murine model. Ectopic bone induced by 5 μg rhBMP-2 delivered by SAIB was quantified by μ-CT. The effects of incorporating 2% (w/v) TCP or BG ± 1 μg ZA were assessed based on BV (Figure 1).

TCP and TCP + ZA did not significantly influence the volume of bone produced, compared to SAIB-rhBMP-2 controls (−30%, p = 0.2743, and +33%, p = 0.3121, respectively). BG alone also did not augment bone formation (−43%, p = 0.1728); however, BG + ZA led to an increase that was significant versus BG alone (p < 0.05), but not versus SAIB-rhBMP-2 controls. X-ray images of representative samples with the median BV values per group are shown in Figure 1(b).

### Bioceramic composition and particle size influence ZA binding

The effects of TCP and BG addition on SAIB-rhBMP-2-induced bone formation were significantly less than those seen with HA,[9] and TCP in particular showed a lack of synergy with ZA addition. It was previously demonstrated that HA could bind and sequester ZA,[9] so comparable ^{14}C-ZA binding assays were undertaken with TCP and BG. HA was included as a control, where both micro-HA and nano-HA were tested.

Following incubation with 50 μM ^{14}C-ZA, the ceramics TCP and BG bound 12% and 6%, respectively (Figure 2). Consistent with prior results,[9] nano-HA bound 92% of ^{14}C-ZA, while micro-HA bound 43%. Notably, both particle sizes of HA were able to bind more ^{14}C-ZA than TCP or BG (p < 0.05 for all comparisons).

Figure 2. Binding affinity of radiolabelled ZA (^{14}C-ZA) is much stronger for either size of HA than TCP or BG. A total of 50 μM of ^{14}C-ZA was added to the ceramics, and the percentage that had bound to the ceramic was quantified using scintillation.
$*p < 0.05$.

As a functional test for bisphosphonate sequestration, an established cell culture assay of ZA-mediated cytotoxicity was utilised.[9] MC3T3 cells were cultured in the presence or absence of 50 μM ZA, with and without TCP or BG (Figure 3(a)) or nano-HA or micro-HA (Figure 3(b)). In wells without ZA, the addition of TCP alone led to a 33% reduction in the numbers of viable cells compared to untreated controls, and BG led to a 27% reduction. In contrast, nano-HA and micro-HA alone had little effect on the growth of cells (95% and 101% of cell control, respectively).
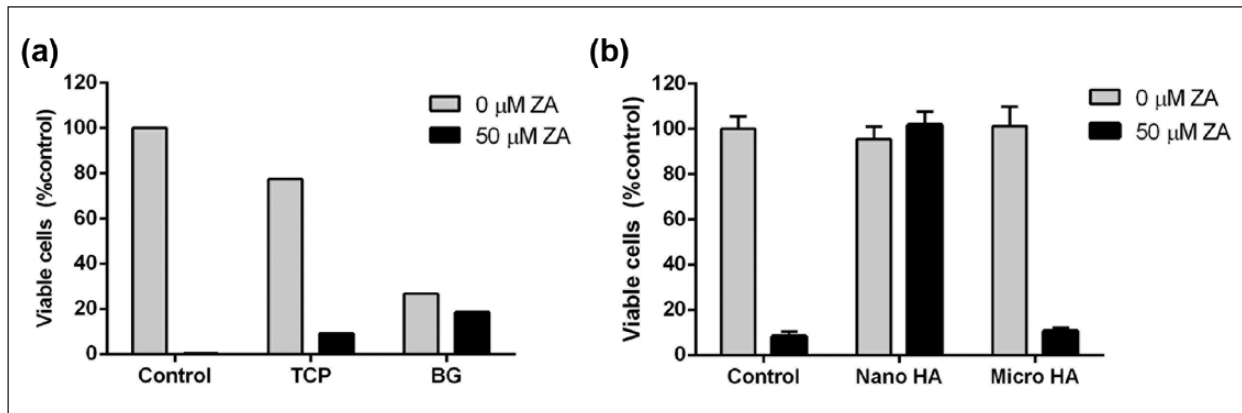
Figure 3. Cultures of MC3T3 cells reveal that the addition of TCP and BG alone reduced cell viability, and only nano-HA is able to rescue cell viability in the presence of 50 μM ZA. Viability is presented as live cells a percentage of the control MC3T3 group, as measured by flow cytometry: with and without (a) TCP or BG and (b) nano-HA or micro-HA.

In wells with 50 μM ZA, considerable cell death was seen at day 7. Consistent with previous results, nano-HA rescued the ZA-treated cells (102% of untreated controls).[9] However, micro-HA was less effective (11% of controls), with no difference significant compared to 50 μM ZA-treated cells. TCP particles led to no rescue of the 50 μM ZA-treated cells, consistent with ^{14}C-ZA binding data. BG particles showed a trend towards increased cell survival with ZA treatment; however, interpretation was confounded by the decreased cell numbers seen with BG alone.

Enhancement of SAIB-rhBMP-2-induced bone with ZA or nano-HA

Based upon the prior in vitro data, the two sizes of HA particles (nano-HA and micro-HA) were compared in a SAIB-rhBMP-2 injection model in rats. A technical advantage of this model was that a larger gauge needle could be employed, which enabled more consistent injection (particularly with the micro-HA groups). A detailed analysis of extrusion force required for different needle gauges is available as supplementary data (Supplementary Figure 1).

Ectopic bone formation induced by 5 μg rhBMP-2 in SAIB was tested with nano-HA versus micro-HA, with and without 2 μg ZA. BV was quantified by μ-CT (Figure 4(a)). Addition of both particle sizes of HA led to significant increase in BV compared to SAIB-rhBMP-2 controls (nano-HA: +126%, $p < 0.05$; micro-HA: +278%, $p < 0.05$). Co-delivery of ZA with HA particles led to further increases in BV versus SAIB-rhBMP-2 controls (nano-HA: +889%, $p < 0.05$; micro-HA: +530%, $p < 0.05$). Conspicuously, nano-HA, which had been previously shown to significantly bind ZA, showed a 337% increase in BV with ZA adsorption. In contrast, micro-HA showed a trend towards an increase in BV with ZA (+66%), but this did not reach statistical significance. Representative X-ray images are presented in Figure 4(b).
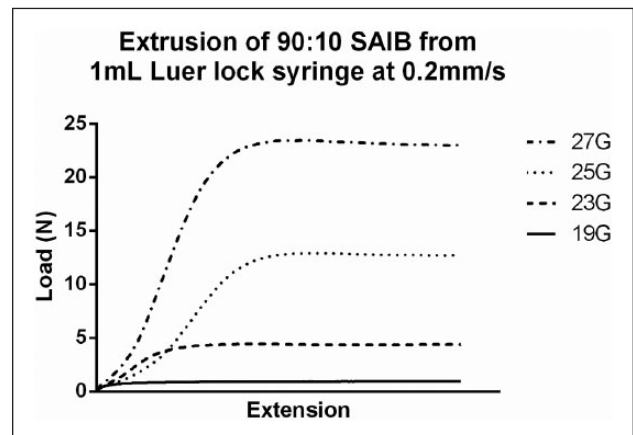

Supplementary Figure 1. Extrusion of a 90:10 SAIB:ethanol dilution through a range of needle gauge sizes highlights the increasing force required to extrude the SAIB mixture through smaller needle sizes.

Nano-HA leads to increased TRAP+ cells

Sections from the centre of the bone nodule underwent a fluorescent TRAP stain and counterstained in DAPI (Figure 5, upper panels). Qualitative inspection indicated increased levels of TRAP staining with nano-HA but not micro-HA. The orientation of the nodules in the fluorescent images can be inferred from haematoxylin and eosin–stained adjacent sections (Figure 5, lower panels). Histological stains also reveal increased retention of trabecular-like bone in the interior of the ectopic bone nodules in HA-ZA-treated samples.

Discussion

In this study, we examined the addition of bioceramic particles of different sizes and compositions to an injectable bone tissue engineering formulation of SAIB-rhBMP-2.
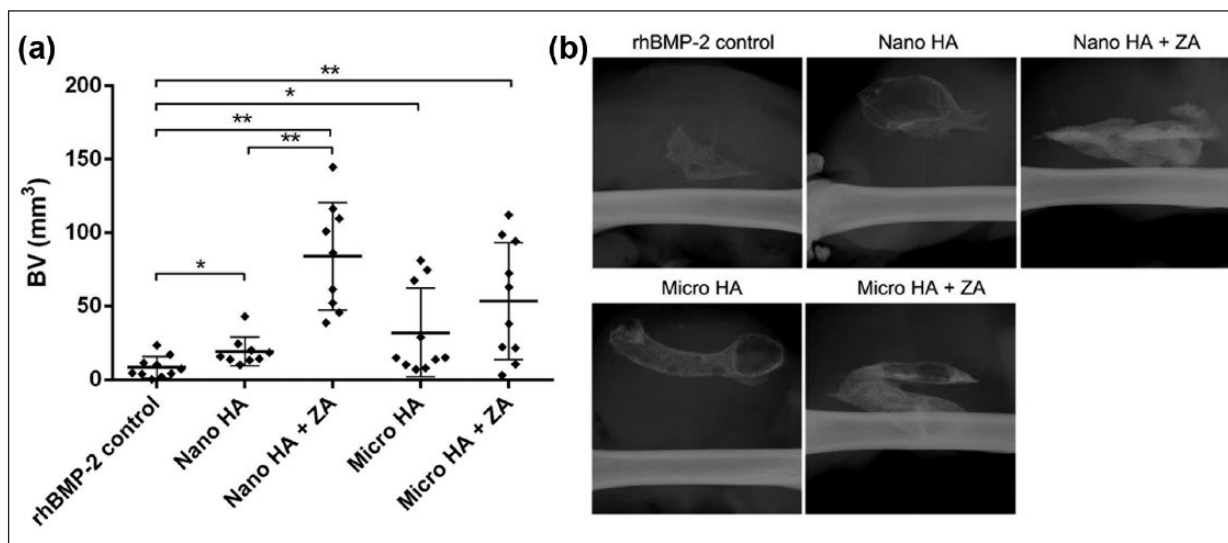
Figure 4. Ectopic bone nodules formed in a rat muscle pouch model in response to 5 μg rhBMP-2 reveal significant increases in bone formation with the addition of either nanoparticle- or microparticle-sized HA and even further increases in bone formation with the co-delivery of ZA: (a) quantification of bone nodules formed in each group via μ-CT and (b) representative X-rays reveal increased radiographic opacity in ZA-containing groups.
*$p < 0.05$; **$p < 0.01$.
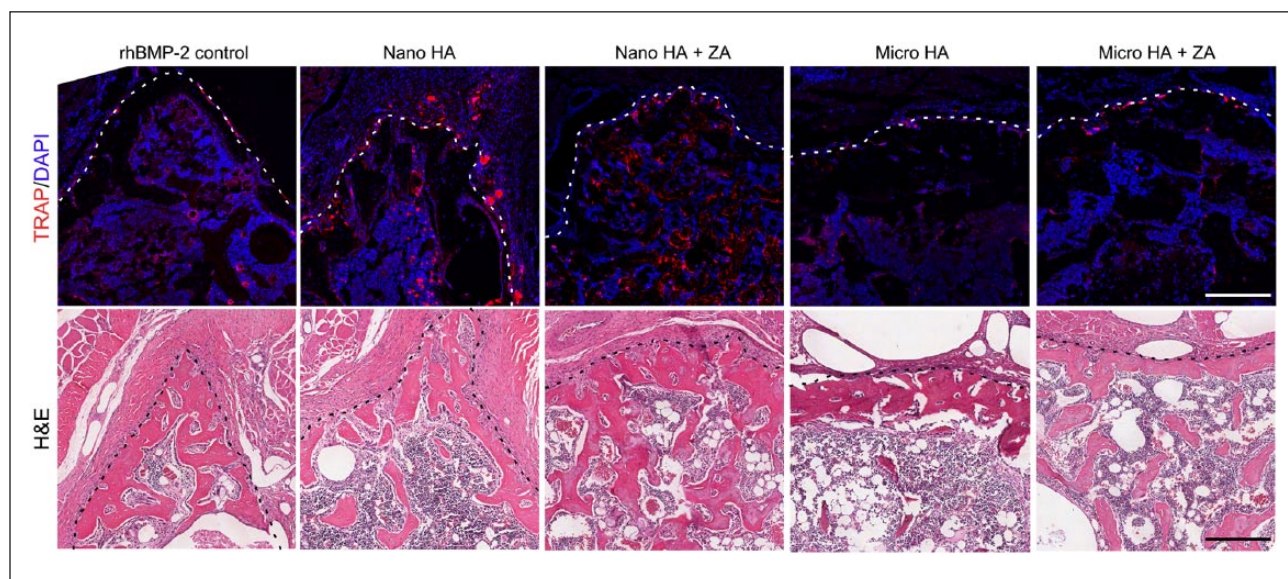
Figure 5. Fluorescent TRAP staining of bone nodules reveals increased TRAP positive cell staining when nanoparticle-sized HA was delivered alongside 5 μg rhBMP-2 in SAIB. Top panels show fluorescent TRAP (red), counterstained with DAPI (blue), and the bottom panels show nearby sections embedded in paraffin and stained with haematoxylin and eosin conducted on representative samples. Dotted line represents the bone pellet border with the muscle pouch (above). Scale bar: 250 μm for all panels.

The effects of pre-adsorbing ZA to the particles were also examined. The addition of TCP and BG led to no significant increases in BV in the murine model. This was in contrast to our prior study using nano-HA that utilised identical methodology.[9] There are conflicting studies within the literature on osteoinductive potential of β-TCP,[32–34] but it is noteworthy that its degradation products can cause inflammation and impair subsequent bone formation.[35]

Prior studies have indicated that BG is not highly osteoinductive de novo,[36] but our study tested it in the context of a potent rhBMP-2 bone formation scenario. Aside from the lack of increased bone seen with TCP and BG alone, neither bioceramic showed significant synergy in combination with a bisphosphonate. This caused us to speculate that a lack of ZA binding may underlie this phenomenon.

The ^{14}C-ZA binding assay is an extremely sensitive assay for measuring the affinity of the interaction between the bisphosphonate and a bioceramic. Such assays can be challenging for ZA compared to other bisphosphonates due to the potency of ZA and the low concentrations it is used at. The binding ^{14}C-ZA to TCP and BG microparticles was significantly less than previously observed for nano-HA,[9] and it was thus speculated that differences in the surface area for bisphosphonate binding could be influencing the results. To test the particle size hypothesis while controlling for the same biomaterial, nano-HA and micro-HA were compared head to head. Both particle sizes of HA showed significantly higher sequestration of ^{14}C-ZA than TCP and BG particles, despite the micro-HA particles being larger by an order of magnitude. Bisphosphonates have a high affinity for bone mineral and the nitrogen-containing bisphosphonates act by inhibiting the enzyme farnesyl pyrophosphate (FPP) synthase.[37–39] These data show that for ZA, the 'bone hook' component of the inhibitor shows a higher affinity for mineral intrinsic to bone (hydroxyapatite) than TCP and BG as bone graft substitutes. This finding has important implications for the uses of these biomaterials in conjunction with bisphosphonates. Nevertheless, it is acknowledged that this study has examined only a single bisphosphonate (ZA); this result would be strengthened by a comparison using other bisphosphonates.

The sequestration of ZA by HA was effectively demonstrated in a biological setting using a cell culture model where MC3T3-E1 osteoblasts are exposed to lethal doses of bisphosphonate (50 μM ZA). We have previously shown that incubation with nano-HA in a transwell was able to bind ZA and prevent cell death.[9] This finding with nano-HA was independently reproduced in this study, but micro-HA, TCP and BG were not able to affect rescue in this assay system. This finding is consistent with the low in vitro binding seen in the ^{14}C-ZA assay, but the negative effects of the alternative bioceramics on cell survival in the absence of ZA were also notable. This may be due to the production of a basic extracellular environment as these bioceramics solubilised over time.[40]

This study concluded with a comparison of the SAIB-rhBMP-2 tissue engineering system in a rat model where both nano-HA and micro-HA were compared. This model was selected both due to technical challenges associated with small volume or small gauge needle injection and to confirm that this formulation was effective in an alternative species. Subsequent studies will need to be performed in large animal models, as it has been well noted that the magnitude of treatment responses tends to decrease in such models.[41] Nonetheless, this study was able to replicate the findings of our previous study using this formulation in mice,[9] reconfirming that nano-HA or ZA gave approximately a 10-fold increase in bone over SAIB-rhBMP-2 alone. Moreover, SAIB-rhBMP-2 has already been reported to produce up to threefold more bone than acellular collagen scaffold (ACS)-rhBMP-2 as the current clinical delivery system.[9]

A final prominent observation was an increase in TRAP+ cells in the nano-HA group via histology. Nano-HA has been previously associated with an increase in osteoclast-like cells when compared to a larger particle sizes in vitro.[42] Moreover, a study that investigated particle sizes of a HA-TCP mixture in rat drill holes found that the smallest particle size (10–20 μm) induced not only the strongest inflammatory response but also the highest new BV.[43] Thus, it could be postulated that nano-HA may yield increased bone formation linked with inflammation but that the associated increases in resorption can be attenuated by pre-adsorption of bisphosphonate.

Conclusion

Our data indicate that the prior synergy seen with nano-HA or ZA with the SAIB-rhBMP-2 delivery system is highly specific for that bioceramic. Alternative bioceramics TCP and BG showed poor in vivo bone formation, low bisphosphonate binding and negligible cytoprotective effects against high-dose ZA in culture. TCP and BG also decreased numbers of viable cells even in the absence of a bisphosphonate, unlike nano-HA and micro-HA particles. In a rat SAIB-rhBMP-2-induced bone formation model, ZA was found to produce more bone in combination with nano-HA, comparable to our prior findings in mice. This was speculated to be due to an increased inflammatory response and bisphosphonate binding compared to micro-HA.

References

1. Meijer GJ, de Bruijn JD, Koole R, et al. Cell-based bone tissue engineering. *PLoS Med* 2007; 4(2): e9.
2. McKay WF, Peckham SM and Badura JM. A comprehensive clinical review of recombinant human bone morphogenetic

protein-2 (INFUSE® Bone Graft). *Int Orthop* 2007; 31(6): 729–734.

3. Fassbender M, Minkwitz S, Strobel C, et al. Stimulation of bone healing by sustained bone morphogenetic protein 2 (BMP-2) delivery. *Int J Mol Sci* 2014; 15(5): 8539–8552.

4. Itoh K, Udagawa N, Katagiri T, et al. Bone morphogenetic protein 2 stimulates osteoclast differentiation and survival supported by receptor activator of nuclear factor-kappaB ligand. *Endocrinology* 2001; 142(8): 3656–3662.

5. Axelrad TW, Steen B, Lowenberg DW, et al. Heterotopic ossification after the use of commercially available recombinant human bone morphogenetic proteins in four patients. *J Bone Joint Surg Br* 2008; 90(12): 1617–1622.

6. Shields LBE, Raque GH, Glassman SD, et al. Adverse effects associated with high-dose recombinant human bone morphogenetic protein-2 use in anterior cervical spine fusion. *Spine* 2006; 31(5): 542–547.

7. Schmitt C, Lutz R, Doering H, et al. Bio-Oss® blocks combined with BMP-2 and VEGF for the regeneration of bony defects and vertical augmentation. *Clin Oral Implants Res* 2013; 24(4): 450–460.

8. Zhang W, Wang X, Wang S, et al. The use of injectable sonication-induced silk hydrogel for VEGF(165) and BMP-2 delivery for elevation of the maxillary sinus floor. *Biomaterials* 2011; 32(35): 9415–9424.

9. Cheng TL, Valtchev P, Murphy CM, et al. A sugar-based phase-transitioning delivery system for bone tissue engineering. *Eur Cell Mater* 2013; 26: 208–221; discussion 220–221.

10. Lin X, Yang S, Gou J, et al. A novel risperidone-loaded SAIB-PLGA mixture matrix depot with a reduced burst release: effects of solvents and PLGA on drug release behaviors in vitro/in vivo. *J Mater Sci Mater Med* 2012; 23(2): 443–455.

11. Reynolds RC and Chappel CI. Sucrose acetate isobutyrate (SAIB): historical aspects of its use in beverages and a review of toxicity studies prior to 1988. *Food Chem Toxicol* 1998; 36(2): 81–93.

12. Hadj A, Hadj A, Hadj A, et al. Safety and efficacy of extended-release bupivacaine local anaesthetic in open hernia repair: a randomized controlled trial. *ANZ J Surg* 2012; 82(4): 251–257.

13. Okumu FW, Dao le N, Fielder PJ, et al. Sustained delivery of human growth hormone from a novel gel system: SABER. *Biomaterials* 2002; 23(22): 4353–4358.

14. Little DG, Ramachandran M and Schindeler A. The anabolic and catabolic responses in bone repair. *J Bone Joint Surg Br* 2007; 89(4): 425–433.

15. Murphy CM, Schindeler A, Gleeson JP, et al. A collagen-hydroxyapatite scaffold allows for binding and co-delivery of recombinant bone morphogenetic proteins and bisphosphonates. *Acta Biomater* 2014; 10(5): 2250–2258.

16. Bosemark P, Isaksson H and Tagil M. Influence of systemic bisphosphonate treatment on mechanical properties of BMP-induced calluses in a rat fracture model: comparison of three-point bending and twisting test. *J Orthop Res* 2014; 32(5): 721–726.

17. Doi Y, Miyazaki M, Yoshiiwa T, et al. Manipulation of the anabolic and catabolic responses with BMP-2 and zoledronic acid in a rat femoral fracture model. *Bone* 2011; 49(4): 777–782.

18. Vaccaro AR. The role of the osteoconductive scaffold in synthetic bone graft. *Orthopedics* 2002; 25(5): S571–S578.

19. Oonishi H. Orthopaedic applications of hydroxyapatite. *Biomaterials* 1991; 12(2): 171–178.

20. Hacking SA, Tanzer M, Harvey EJ, et al. Relative contributions of chemistry and topography to the osseointegration of hydroxyapatite coatings. *Clin Orthop Relat Res* 2002; 405: 24–38.

21. Epinette J-A. Long lasting outcome of hydroxyapatite-coated implants in primary knee arthroplasty: a continuous series of two hundred and seventy total knee arthroplasties at fifteen to twenty two years of clinical follow-up. *Int Orthop* 2014; 38(2): 305–311.

22. Yano K, Namikawa T, Uemura T, et al. Regenerative repair of bone defects with osteoinductive hydroxyapatite fabricated to match the defect and implanted with combined use of computer-aided design, computer-aided manufacturing, and computer-assisted surgery systems: a feasibility study in a canine model. *J Orthop Sci* 2012; 17(4): 484–489.

23. Van Hoff C, Samora JB, Griesser MJ, et al. Effectiveness of ultraporous β-tricalcium phosphate (vitoss) as bone graft substitute for cavitary defects in benign and low-grade malignant bone tumors. *Am J Orthop* 2012; 41(1): 20–23.

24. Trombelli L, Franceschetti G, Stacchi C, et al. Minimally invasive transcrestal sinus floor elevation with deproteinized bovine bone or β-tricalcium phosphate: a multicenter, double-blind, randomized, controlled clinical trial. *J Clin Periodontol* 2014; 41(3): 311–319.

25. Harel N, Moses O, Palti A, et al. Long-term results of implants immediately placed into extraction sockets grafted with β-tricalcium phosphate: a retrospective study. *J Oral Maxillofac Surg* 2013; 71(2): e63–e68.

26. Stavropoulos A, Sima C, Sima A, et al. Histological evaluation of healing after transalveolar maxillary sinus augmentation with bioglass and autogenous bone. *Clin Oral Implants Res* 2012; 23(1): 125–131.

27. Chacko NL, Abraham S, Rao HNS, et al. A clinical and radiographic evaluation of periodontal regenerative potential of PerioGlas®: a synthetic, resorbable material in treating periodontal infrabony defects. *J Int Oral Health* 2014; 6(3): 20–26.

28. Gauthier O, Bouler JM, Weiss P, et al. Short-term effects of mineral particle sizes on cellular degradation activity after implantation of injectable calcium phosphate biomaterials and the consequences for bone substitution. *Bone* 1999; 25(2): 71S–74S.

29. Yu NYC, Schindeler A, Peacock L, et al. Modulation of anabolic and catabolic responses via a porous polymer scaffold manufactured using thermally induced phase separation. *Eur Cell Mater* 2013; 25: 190–203.

30. Yu NYC, Gdalevitch M, Murphy CM, et al. Spatial control of bone formation using a porous polymer scaffold co-delivering anabolic rhBMP-2 and anti-resorptive agents. *Eur Cell Mater* 2014; 27: 98–111.

31. Schindeler A and Little DG. Osteoclasts but not osteoblasts are affected by a calcified surface treated with zoledronic acid in vitro. *Biochem Biophys Res Commun* 2005; 338(2): 710–716.

32. Kim C-S, Kim J-I, Kim J, et al. Ectopic bone formation associated with recombinant human bone morphogenetic

proteins-2 using absorbable collagen sponge and beta tricalcium phosphate as carriers. *Biomaterials* 2005; 26(15): 2501–2507.

33. Neo M, Herbst H, Voigt CF, et al. Temporal and spatial patterns of osteoblast activation following implantation of β-TCP particles into bone. *J Biomed Mater Res* 1998; 39(1): 71–76.

34. Gatti AM, Zaffe D and Poli GP. Behaviour of tricalcium phosphate and hydroxyapatite granules in sheep bone defects. *Biomaterials* 1990; 11(7): 513–517.

35. Hing KA, Wilson LF and Buckland T. Comparative performance of three ceramic bone graft substitutes. *Spine J* 2007; 7(4): 475–490.

36. Metzler P, von Wilmowsky C, Zimmermann R, et al. The effect of current used bone substitution materials and platelet-rich plasma on periosteal cells by ectopic site implantation: an in-vivo pilot study. *J Cranio-Maxillofac Surg* 2012; 40(5): 409–415.

37. Coxon FP, Thompson K, Roelofs AJ, et al. Visualizing mineral binding and uptake of bisphosphonate by osteoclasts and non-resorbing cells. *Bone* 2008; 42(5): 848–860.

38. Rogers MJ, Crockett JC, Coxon FP, et al. Biochemical and molecular mechanisms of action of bisphosphonates. *Bone* 2011; 49(1): 34–41.

39. Rogers MJ, Gordon S, Benford H, et al. Cellular and molecular mechanisms of action of bisphosphonates. *Cancer* 2000; 88(Suppl. 12): 2961–2978.

40. Silver IA, Deas J and Erecińska M. Interactions of bioactive glasses with osteoblasts in vitro: effects of 45S5 Bioglass®, and 58S and 77S bioactive glasses on metabolism, intracellular ion concentrations and cell viability. *Biomaterials* 2001; 22(2): 175–185.

41. Termaat MF, Den Boer FC, Bakker FC, et al. Bone morphogenetic proteins: development and clinical efficacy in the treatment of fractures and bone defects. *J Bone Joint Surg Am* 2005; 87(6): 1367–1378.

42. Webster TJ, Ergun C, Doremus RH, et al. Enhanced osteoclast-like cell functions on nanophase ceramics. *Biomaterials* 2001; 22(11): 1327–1333.

43. Malard O, Bouler JM, Guicheux J, et al. Influence of biphasic calcium phosphate granulometry on bone ingrowth, ceramic resorption, and inflammatory reactions: preliminary in vitro and in vivo study. *J Biomed Mater Res* 1999; 46(1): 103–111.